JBC ARTICLE

Lysine acetylation of F-actin decreases tropomyosin-based inhibition of actomyosin activity

Received for publication, July 20, 2020, and in revised form, August 18, 2020 Published, Papers in Press, September 1, 2020, DOI 10.1074/jbc.RA120.015277

William Schmidt, Aditi Madan, D. Brian Foster, and Anthony Cammarato*

From the Department of Medicine, Johns Hopkins University School of Medicine, Baltimore, Maryland, USA

Edited by Enrique M. De La Cruz

Recent proteomics studies of vertebrate striated muscle have identified lysine acetylation at several sites on actin. Acetylation is a reversible post-translational modification that neutralizes lysine's positive charge. Positively charged residues on actin, particularly Lys^{326} and Lys^{328}, are predicted to form critical electrostatic interactions with tropomyosin (Tpm) that promote its binding to filamentous (F)-actin and bias Tpm to an azimuthal location where it impedes myosin attachment. The troponin (Tn) complex also influences Tpm's position along F-actin as a function of Ca^{2+} to regulate exposure of myosin-binding sites and, thus, myosin cross-bridge recruitment and force production. Interestingly, Lys^{326} and Lys^{328} are among the documented acetylated residues. Using an acetic anhydride-based labeling approach, we showed that excessive, nonspecific actin acetylation did not disrupt characteristic F-actin–Tpm binding. However, it significantly reduced Tpm-mediated inhibition of myosin attachment, as reflected by increased F-actin–Tpm motility that persisted in the presence of Tn and submaximal Ca^{2+}. Furthermore, decreasing the extent of chemical acetylation, to presumptively target highly reactive Lys^{326} and Lys^{328}, also resulted in less inhibited F-actin–Tpm, implying that modifying only these residues influences Tpm's location and, potentially, thin filament regulation. To unequivocally determine the residue-specific consequences of acetylation on Tn–Tpm–based regulation of actomyosin activity, we assessed the effects of K326Q and K328Q acetyl (Ac)-mimetic actin on Ca^{2+}-dependent, *in vitro* motility parameters of reconstituted thin filaments (RTFs). Incorporation of K328Q actin significantly enhanced Ca^{2+} sensitivity of RTF activation relative to control. Together, our findings suggest that actin acetylation, especially Lys^{328}, modulates muscle contraction via disrupting inhibitory Tpm positioning.

Muscle contraction is driven by cyclical, force-generating interactions between myosin-containing thick and actin-based thin filaments (1, 2). Conversely, relaxation occurs when actomyosin binding is inhibited and/or suppressed by Tn and Tpm on thin filaments, or by the sequestration of myosin heads on thick filaments (1–4). Tn is a trimer composed of inhibitory (TnI), Tpm-binding (TnT), and Ca^{2+}-binding (TnC) subunits (1, 2, 5). Each Tn–Tpm holoregulatory complex associates with seven actin protomers of the thin filament to confer Ca^{2+} sensitivity of contraction (1, 2). Under low Ca^{2+}, TnI restricts Tpm to the blocked "B-state" position along F-actin where it sterically inhibits myosin binding (1, 2, 5). This effect is attenuated as free intracellular Ca^{2+} rises and binds to TnC. Ca^{2+}-TnC binding relieves TnI-mediated constraints on Tpm and facilitates its azimuthal movement to the closed "C-state," partial exposure of myosin-binding sites on actin, and weak myosin binding. The transition of myosin heads from a weak to strong F-actin-bound state induces additional Tpm movement to the open "M-state," triggering cooperative thin filament activation and force generation. Hence, contraction demands both Tn- and myosin-dependent shifts in Tpm position.

Tpm is an α-helical, coiled-coil dimer consisting of seven tandem "quasi-equivalent," pseudorepeating motifs that bind adjacent actin monomers (6–8). It self-polymerizes head to tail to form a continuous cable that extends the entire length of F-actin (9–13). Tpm dimers individually bind with weak affinity, orchestrated by favorable electrostatic contacts between residues of each actin protomer and Tpm pseudorepeat, yet the polymerized cable binds with exceedingly high affinity (10, 14–19). This contrasting behavior, described as "gestalt-binding," bestows on Tpm the requisite ability to easily shift its azimuthal position over the F-actin surface to regulate myosin binding to the thin filament without risk of catastrophic detachment (10, 20). Mutations that disrupt the weak, local binding of Tpm to F-actin, as suggested by distorted, computationally derived F-actin–Tpm electrostatic energy landscapes, may minimally impact F-actin–Tpm global binding affinity yet elicit significant changes in Tpm's ability to properly impede actomyosin binding and cross-bridge cycling (21–23). Therefore, perturbed F-actin–Tpm electrostatic interactions could affect Tpm's preferred binding position and/or its regulatory switching between the B-, C-, and M-states along F-actin and, thus, Tpm-mediated regulation of actomyosin activity.

EM reconstructions and *in silico*-generated atomic models of Tpm bound to F-actin have identified Tpm's potential default Apo- or "A-state" binding location, where the regulatory strand is positioned such that it sterically hinders myosin binding in the absence of Tn (12, 15, 20, 24). Lys^{326} and Lys^{328} of actin are predicted to form highly favorable electrostatic contacts with Tpm and stabilize its native inhibitory configuration (12, 15, 17–19, 25, 26). These associations dominate the computed F-actin–Tpm interaction energy landscape and, together with TnI-actin interactions, are essential for establishing the B-state (5, 12, 15, 22, 27). Modification or mutation of Lys^{326} or Lys^{328}

This article contains supporting information.

* For correspondence: Anthony Cammarato, acammar3@jhmi.edu.

Present address for William Schmidt: Rivier University, Science and Innovation Center, Nashua, New Hampshire, USA.

on actin or residues in their vicinity has been shown to alter contractile regulation and induce cardiac and skeletal myopathies (21, 22, 28–30).

Recently, 10 distinct lysines of actin were identified as targets of acetylation in independent proteomics assessments of healthy, vertebrate cardiac and skeletal muscle (31, 32). Of those 10 residues, 5, including Lys^{326} and Lys^{328}, were reported to be acetylated in both studies. Lysine acetylation is a reversible post-translational modification (PTM) where the transfer of an Ac group to the residue's side-chain terminal amine neutralizes its positive charge. Because Lys^{326} and Lys^{328} on actin are likely critical for establishing favorable electrostatic interactions with Tpm, "masking" the charges could destabilize F-actin–Tpm binding and/or inhibitory positioning, resulting in increased actomyosin cross-bridge formation and enhanced force production. In fact, mimicking acetylation by replacing the charged lysines at positions 326 and 328 with uncharged glutamines in *Drosophila* indirect flight muscle (IFM) altered flight ability and stimulated IFM fiber destruction because of excessive, myosin-dependent force generation (30).

In vivo, actin acetylation levels may be distinctly modulated. For example, fluctuations in intracellular concentrations of Ac-CoA stimulate changes in lysine acetylation levels via mass action (33, 34). Alternatively, enzymatic-mediated changes in acetylation require targeting of actin by particular lysine acetylase(s) (KATs) and/or deacetylase(s) (KDACs). Despite evidence implicating specific enzymes that may perform this role *in vivo* (35–37), to the best of our knowledge no group has provided evidence of successful enzymatic acetylation of purified, sarcomeric actin *in vitro*. On the other hand, *in vitro* chemical acetylation of actin is eminently feasible (38–40). For example, Hitchcock-DeGregori *et al.* discovered, via a competitive labeling method, that Lys^{326} and Lys^{328} on F-actin displayed a high propensity for acetylation and were preferentially modified relative to all other lysines (38).

Here, we hypothesize that actin Lys^{326} and/or Lys^{328} acetylation decreases Tpm-based inhibition of myosin binding by direct disruption of F-actin–Tpm electrostatic contacts and resultant Tpm mispositioning, which ultimately manifests as enhanced Ca^{2+} sensitivity in regulated thin filaments. To test our hypothesis, we implemented a two-pronged approach that determined the effects of 1) indiscriminate and probabilistic, but preferential, actin lysine acetylation on global F-actin–Tpm binding and on the inherent inhibitory positioning of Tpm along F-actin in the absence and presence of Tn and 2) residue-specific pseudoacetylation of Lys^{326} or Lys^{328} on Ca^{2+}-mediated regulation of RTFs. Our results suggest that although Lys^{326} and Lys^{328} acetylation does not affect collective F-actin–Tpm affinity, Lys^{328} acetylation does lessen Tpm's intrinsic ability to inhibit myosin cross-bridge binding, which contributes to enhanced thin filament Ca^{2+} sensitivity.

Results

According to the Behrmann *et al.* (41) F-actin–Tpm–myosin rigor structure, Lys^{328} of actin forms a salt bridge with Glu^{286} of myosin (Fig. 1*A*). Acetylation of Lys^{328} and masking of its positive charge would predictably disrupt this interaction, which could potentially affect myosin binding and/or cross-bridge cycling. We pan-acetylated F-actin with acetic anhydride to increase actin-normalized lysine acetylation levels ~290-fold (Fig. 1, *B* and *C*, and Fig. S1) and employed *in vitro* motility assays to assess its gross effect on actomyosin interactions (Fig. 1*D*). Sliding velocities of control and acetylated F-actin did not significantly differ at any of the myosin concentrations tested, suggesting that, in general, actomyosin cross-bridge cycling is seemingly unaffected by actin acetylation.

To rule out the possibility that the lack of an effect on F-actin sliding velocities was because Lys^{328} remained unmodified, we employed MS to confirm which lysines were acetylated following chemical treatment (Table 1). Specifically, MS detected 22 unique spectral matches to 19 unique tryptic peptide sequences. These corresponded to 12 distinct acetylation sites, most of which are common to multiple actin gene products, including cardiac, skeletal, and cytoplasmic isoforms. Lys^{328} acetylation was confirmed. Therefore, the absence of an acetylation-induced effect on actomyosin cycling, and specifically F-actin propulsion speeds, could not be attributed to a failure of Lys^{328} to be chemically modified *in vitro*.

Lys^{326} and Lys^{328} of seven consecutive actin protomers are predicted to interact with negatively charged residues of every pseudorepeat along Tpm's entire length (12, 15, 20, 25, 26) (Fig. 2*A*). Previously, site-directed mutagenesis of Asp^{25}, Glu^{334}, Lys^{326}, and Lys^{328} of human smooth muscle actin was shown to result in a complete loss of bacterially expressed Tpm binding, which suggests that the lysines may contribute to global F-actin–Tpm binding (19). Therefore, we determined the effect of F-actin acetylation on the binding of tissue-purified cardiac Tpm via co-sedimentation (Fig. S2). We postulated that modifying the preponderance of actin lysines, especially Lys^{326} and Lys^{328}, would potentially decrease maximum F-actin–Tpm binding (B_{max}) and/or affinity (K_d). However, B_{max} and K_d of Tpm for control (B_{max} = 0.15 ± 0.01; K_d = 0.21 ± 0.03 μM) and acetylated (B_{max} = 0.14 ± 0.01; K_d = 0.15 ± 0.04 μM) F-actin did not significantly differ (Fig. 2*B*). Thus, extensive chemical modification of actin lysines did not appear to alter either the number of available Tpm-binding sites or the affinity of the polymerized Tpm cable for F-actin.

It is well-established that F-actin–Tpm association is highly influenced by buffer ionic strength because of the considerable contribution of electrostatic interactions to binding (42–44). Therefore, actin acetylation may alter the buffer salt sensitivity of Tpm binding because of marked reduction in positively charged lysines, specifically Lys^{326} and/or Lys^{328}. We performed F-actin–Tpm co-sedimentation assays at varying KCl concentrations to determine whether actin acetylation modifies the effect of buffer salt on F-actin–Tpm binding (Fig. 2*C*). At 40 and 200 mM KCl, control (112 ± 6.3 and 85.4 ± 6.9%, respectively) and acetylated (113 ± 2.2 and 70.4 ± 4.7%, respectively) F-actin bound roughly equivalent amounts of Tpm, although increasing KCl concentration to 500 mM and above resulted in a nearly complete lack of Tpm binding to both F-actin types. This supports the idea that despite extensive lysine charge neutralization of acetylated F-actin, including Lys^{326} and Lys^{328}, collective Tpm binding to F-actin remains largely intact.

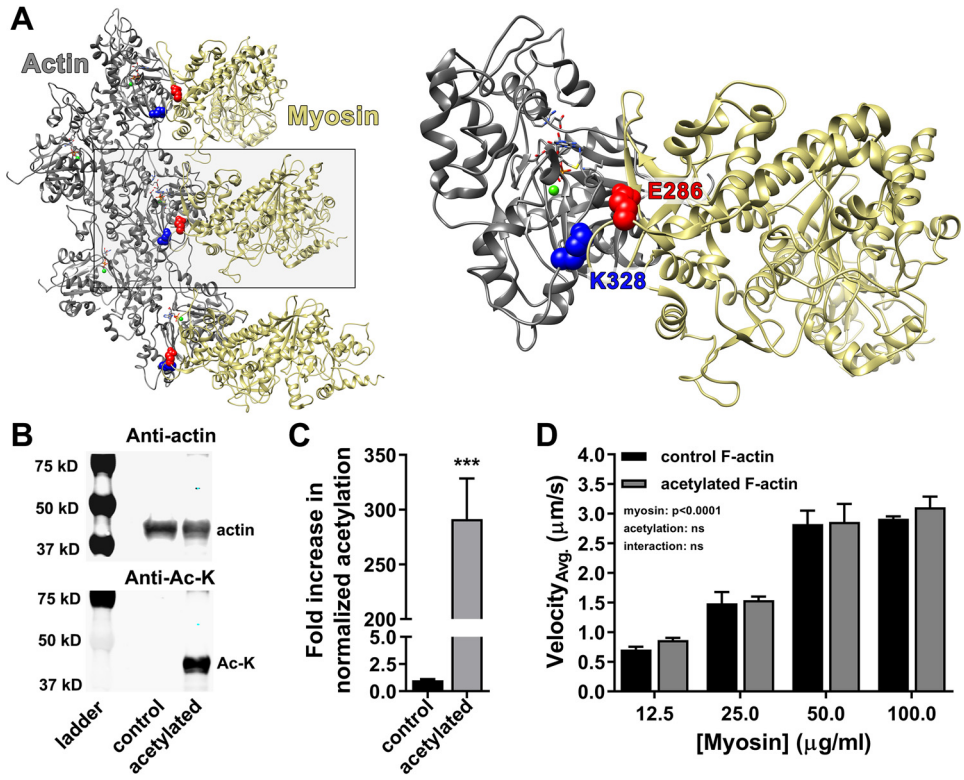

Figure 1. Actin acetylation does not significantly alter myosin-driven F-actin sliding velocity. *A*, proposed Lys^{328}–Glu^{286} (*blue–red*, respectively) actin–myosin (*gray–tan*, respectively) salt bridge established during strong binding (Protein Data Bank code 4A7f) (41). *B*, Western blots of actin treated with supra-stoichiometric acetic anhydride diluted in acetonitrile (acetylated) revealed increased lysine acetylation relative to actin resuspended in acetonitrile only (control). The blots were probed with anti-actin (*top panel*) and anti–Ac-lysine (*bottom panel*; *Anti-Ac-K*) antibodies. *C*, anti–Ac-lysine intensities in *B* were normalized to corresponding anti-actin signals. Actin-normalized lysine acetylation increased ~290-fold (291 ± 37) relative to control. *D*, *in vitro* motility of Alexa 568 Ph-labeled control (*black*) and acetylated (*gray*) F-actin at varying myosin concentrations. Average velocities (Velocity$_{Avg.}$) were not significantly different, suggesting no change in actomyosin cross-bridge cycling caused by actin acetylation (two-way ANOVA; $n = 4$).

Next, we assessed whether Tpm was located along acetylated F-actin at or near its typical inhibitory A-state position and could, therefore, alter actomyosin cycling and/or the extent of myosin recruitment, which influences muscle contraction (45, 46). We first determined *in vitro* motility velocities of control and acetylated F-actin and F-actin–Tpm at varying myosin concentrations (Fig. 3, *A* and *B*). To facilitate interpretation regarding the degree to which Tpm reduces filament gliding speeds, we normalized control and acetylated F-actin–Tpm velocities at each myosin concentration to their respective F-actin velocities, subtracted normalized values from one, and multiplied by 100 to quantify the percentage of Tpm-based inhibition (Fig. 3*C*). As observed previously (47–50), Tpm significantly decreased ($p < 0.0001$) both control (Fig. 3*A*) and acetylated (Fig. 3*B*) F-actin velocities; however, actin acetylation had no significant effect on Tpm-mediated reduction of velocity (Fig. 3*C*). To further assess the effect of Tpm on actomyosin binding, we quantified the percentage of moving control and acetylated actin and actin–Tpm filaments (Fig. 3, *D* and *E*). Consistent with an inhibitory effect on velocity (Fig. 3, *A*–*C*), Tpm significantly decreased ($p < 0.0001$) the percentage of motile control (Fig. 3*D*) and acetylated (Fig. 3*E*) F-actin. However, in contrast, acetylated F-actin–Tpm movement was significantly elevated (*i.e.* less inhibited ($p < 0.0001$)) relative to control (Fig. 3*F*), whereas the PTM, again (Fig. 1*D*), had no impact on F-actin movement (Fig. 3, *D* and *E*). Therefore, Tpm's intrinsic ability to inhibit myosin recruitment to acetylated F-actin, as opposed to cross-bridge turnover rate, was significantly attenuated compared with control F-actin (Fig. 3, *C* and *F*). In addition, the greatest difference (*i.e.* a 63% relative increase) in acetylated *versus* control F-actin–Tpm movement occurred at the lowest myosin concentration tested (12.5 μg/ml). Under these conditions, myosin-dependent, propagated movement of Tpm and exposure of proximal binding sites is normally relatively minimal. Thus, Tpm likely remains predominantly in the A-state along control F-actin, and the extent of myosin binding is determined by Tpm's inherent ability to block myosin attachment, which appears compromised following modification of F-actin lysines. Taken together, the data suggest that actin acetylation increases cross-bridge accessibility by impairing Tpm's capacity to adequately impede actomyosin binding when Tpm alone is bound to F-actin. This effect could potentially translate into less inhibited thin filaments in the presence of Tn and Ca^{2+}.

We subsequently assessed the ability of acetylated actin to serve as the backbone of a filament that responds to Ca^{2+}. We reconstituted thin filaments by adding Tn–Tpm to control and acetylated F-actin and determined the velocity and percentage of moving filaments at three distinct Ca^{2+} levels. Given the more pronounced relative effect of actin acetylation on F-actin–Tpm movement under low myosin concentrations, we

Table 1

Chemically acetylated lysine residues on actin

Actin was acetylated with an 80:1 molar ratio of acetic anhydride:actin, digested with trypsin and analyzed by MS as described under "Experimental procedures." Acetylated peptides were identified by a mass search of *in silico* trypsinized rabbit skeletal actin (UniProt KB-P68135), allowing for variable modification of lysine residues with a mass shift of 42 kDa (71). Annotated spectra associated with each peptide can be found in the supporting information (Fig. S6)

Entry	Acetylated peptide sequence	Modifications	Protein accessions	Protein name	Acetylation site[a]	Peptide identification probability	Acetyl site localization probability[b]	Best Mascot ion score[c]	Mascot identity score[d]	Observed mass	Actual mass	Charge	Δ
						%	%						*ppm*
1	(K)DSYVGDEAQS**k**R(G)	Acetyl (+42)	XP_002722940.1, XP_002718044.1, NP_001095153.1	Actin, Sk, Ca, and Cy	Lys^{61}	100	100	79.84	27.19	698.8216	1,395.63	2	1.354
2	(R)VAPEEHPTLLTEAPLNP**k**ANR(E)	Acetyl (+42)	XP_002722940.1, XP_002718044.1	Actin, Sk, and Ca	Lys^{113}	100	100	78.04	31.45	780.4176	2,338.23	3	1.127
3	(R)DLTDYLM**k**ILTER(X)	Acetyl (+42)	XP_002722940.1, XP_002718044.1, NP_001095153.1	Actin, Sk, Ca, and Cy	Lys^{191}	100	100	51.8	30.77	551.6243	1,651.85	3	1.044
4	(R)DLTDYLm**k**ILTER(X)	Oxidation (+16), acetyl (+42)	XP_002722940.1, XP_002718044.1, NP_001095153.1	Actin, Sk, Ca and Cy	Lys^{191}	100	100	62.48	30.76	834.9309	1,667.85	2	1.676
5	(K)E**k**LcYVALDFENEMATAASSSSLEK(S)	Acetyl (+42), carbamidomethyl (+57)	XP_002722940.1, XP_002718044.1	Actin, Sk, and Ca	Lys^{215}	100	100	109.05	31.86	945.7747	2,834.30	3	1.139
6	(R)cPETLFQPSFIGMESAGIHETTYnSIM**k**(C)	Carbamidomethyl (+57), deamidated (+1), acetyl (+42)	XP_002722940.1, XP_002718044.1	Actin, Sk, and Ca	Lys^{284}	100	100	50.58	31.39	1,077.83	3,230.48	3	4.349
7	(R)**kD**LYANNVMSGGTTmYPGIADR(M)	Acetyl (+42), oxidation (+16)	XP_002722940.1	Actin and Sk	Lys^{291}	100	100	80.92	31.06	811.3799	2,431.12	3	1.209
8	(R)**kD**LYANNV_mSGGTTmYPGIADR(M)	Acetyl (+42), oxidation (+16), oxidation (+16)	XP_002722940.1	Actin and Sk	Lys^{291}	100	100	69.9	31.14	816.7142	2,447.12	3	4.377
9	(R)MQ**k**EITALAPSTMK(I)	Acetyl (+42)	XP_002722940.1, XP_002718044.1, NP_001095153.1	Actin, Sk, Ca, and Cy	Lys^{315}	100	100	56.72	31.49	795.915	1,589.82	2	−0.3323
10	(K)EITALAPSTMKI**k**(I)	Acetyl (+42)	XP_002722940.1, XP_002718044.1, NP_001095153.1	Actin, Sk, Ca, and Cy	Lys^{326}	100	100	59.07	29.24	722.9083	1,443.80	2	0.7138
11	(K)EITALAPSTM**k**I**k**IIAPPER(K)	Acetyl (+42), acetyl (+42)	XP_002722940.1, XP_002718044.1, NP_001095153.1	Actin, Sk, Ca, and Cy	Lys^{326}, Lys^{328}	100	100	36.84	26.92	755.0963	2,262.27	3	0.3617
12	(K)I**k**IIAPPER(K)	Acetyl (+42)	XP_002722940.1, XP_002718044.1, NP_001095153.1	Actin, Sk, Ca, and Cy	Lys^{328}	100	100	51.91	25.00	539.8353	1,077.66	2	1.067
13	(K)IIAPPER**k**YSVWIGGSILASLSTFQQmWITK(Q)	Acetyl (+42), oxidation (+16)	XP_002722940.1	Actin and Sk	Lys^{336}	100	100	18.07	29.25	895.4843	3,577.91	4	1.979
14	(K)IIAPPERKYSVWIGGSILASLSTFQQMWIT**k**qEYDEAGPSIVHR(K)	Acetyl (+42), deamidated (+1)	XP_002722940.1	Actin and Sk	Lys^{359}	100	100	103.97	30.22	1,009.93	5,044.60	5	4.512
15	(R)KYSVWIGGSILASLSTFQqMWIT**k**(Q)	Deamidated (+1), acetyl (+42)	XP_002722940.1	Actin and Sk	Lys^{359}	100	100	43.34	32.46	929.8234	2,786.45	3	4.556
16	(R)**k**YSVWIGGSILASLSTFQQmWITKQEYDEAGPSIVHR(K)	Acetyl (+42), oxidation (+16)	XP_002722940.1	Actin and Sk	Lys^{336}	100	100	56.21	33.57	857.6372	4,283.15	5	3.015
17	(R)KYSVWIGGSILASLSTFQqMWIT**k**QEYDEAGPSIVHR(K)	Deamidated (+1), acetyl (+42)	XP_002722940.1	Actin and Sk	Lys^{359}	100	100	35.18	33.39	854.6355	4,268.14	5	3.646
18	(K)YSVWIGGSILASLSTFQQMWIT**k**qEYDEAGPSIVHR(K)	Acetyl (+42), deamidated (+1)	XP_002722940.1	Actin and Sk	Lys^{359}	100	100	56.21	34.16	1,036.02	4,140.05	4	3.985
19	(R)KYSVWIGGSILASLSTFQQmWI**Sk**QEYDEAGPSIVHR(K)	Oxidation (+16), acetyl (+42)	XP_002718044.1	Actin and Ca	Lys^{359}	100	100	35.64	33.96	1,068.29	4,269.13	4	2.638
20	(R)**kD**LYAnnVLSGGTTMYPGIADR(M)	Acetyl (+42), deamidated (+1), deamidated (+1)	XP_002718044.1	Actin and Ca	Lys^{291}	96	100	16.94	31.74	600.7888	2,399.13	4	−2.33
21	(R)EIVRDIKE**k**LcYVALDFEqEMATAASSSSLEK(S)	Acetyl (+42), carbamidomethyl (+57), deamidated (+1)	NP_001095153.1	Actin and Cy	Lys^{213}	97	100	20.47	34.17	926.7111	3,702.82	4	3.85
22	(K)E**k**LcYVALDFEqEMATAASSSSLEK(S)	Acetyl (+42), carbamidomethyl (+57), deamidated (+1)	NP_001095153.1	Actin and Cy	Lys^{213}	100	100	63.54	32.40	950.7781	2,849.31	3	4.832

[a]Site numbering according to the sequence, *in vivo*, which excludes the first two amino acids that are cleaved post-translationally.
[b]Position of Ac moiety assessed using the A-score algorithm of Beausoleil *et al.* (71).
[c]Ion score = −10log (probability that match is random).
[d]Identity score is the score greater than which peptide identity has $p < 0.05$.

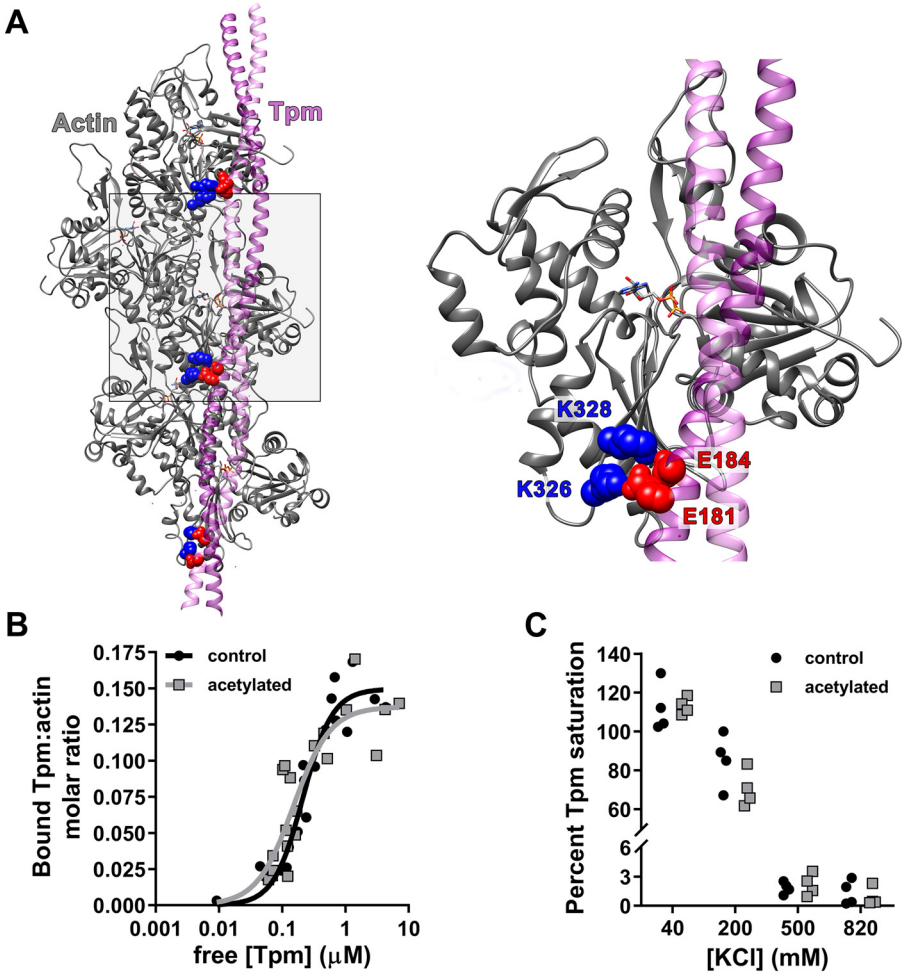

Figure 2. Actin acetylation does not disrupt global F-actin–Tpm binding. *A*, purported contacts between Lys^{326}/Lys^{328} (*blue*) on actin (*gray*) and negatively charged Tpm (*purple*) residues (*red*) in pseudorepeats 4, 5, and 6 (from *bottom* to *top*) (12). *B*, F-actin–Tpm co-sedimentation data were fit to the Hill equation ($y = B_{max} \times x^h/(K_d{}^h + x^h)$), and no significant differences were found in B_{max} or K_d of Tpm for control (*black*; $B_{max} = 0.15 \pm 0.009$; $K_d = 0.21 \pm 0.03$ μM, respectively) *versus* acetylated (*gray*; $B_{max} = 0.14 \pm 0.013$; $K_d = 0.15 \pm 0.04$ μM, respectively) F-actin. *C*, saturating amounts of Tpm were mixed with control (*black*) or acetylated (*gray*) F-actin at 40, 200, 500, and 820 mM [KCl] and pelleted. At 40 mM, the percentage of Tpm saturation of control (112 ± 6.3%) *versus* acetylated (113 ± 2.2%) F-actin was equivalent. Increasing [KCl] to 200 mM similarly decreased Tpm binding to control (85.4 ± 6.85%) and acetylated (70.4 ± 4.68%) F-actin, which was nearly fully ablated by 500 mM.

elected to measure RTF activation at 25 μg/ml myosin. At low Ca^{2+} (pCa 9), movement of control and acetylated actin-containing RTFs was limited and discontinuous and, therefore, unquantifiable under our motion criteria (see supporting information) (Fig. 4*A*). At high Ca^{2+} (pCa 4), the average velocity and percentage of filaments moving of acetylated actin-containing RTFs (1.11 ± 0.17 μM/s and 40.5 ± 3.4%, respectively) were comparable with control (1.19 ± 0.21 μM/s and 40.1 ± 3.9%, respectively) (Fig. 4, *A* and *B*). However, when assessed at a submaximal, activating level of steady-state Ca^{2+} (pCa 6.5), akin to an amount transiently present in actively contracting human myocytes (51–53), average acetylated *versus* control actin-containing RTF velocities (0.27 ± 0.01 μM/s *versus* 0.18 ± 0.02 μM/s, respectively) along with percentage of filaments moving (24.75 ± 1.63% *versus* 20.11 ± 1.45%, respectively) were significantly elevated ($p < 0.05$) (Fig. 4*C*). These results are consistent with enhanced F-actin–Tpm movement (Fig. 3, *D–F*) and indicate that acetylated actin is capable of forming a Ca^{2+}-responsive thin filament that is less inhibited and hypersensitive to Ca^{2+}.

Because Lys^{50}, Lys^{61}, Lys^{315}, Lys^{326}, and Lys^{328} are commonly observed actin acetylation sites in vertebrates (31, 32), they may be the most physiologically relevant. As previously noted, Lys^{326} and Lys^{328} are critical for establishing Tpm's inhibitory state *in vitro* and *in vivo* (12, 15, 20, 22, 30); accordingly, it stands to reason that acetylation of these residues specifically would have the greatest contribution to Tpm mispositioning and increased actomyosin accessibility. Therefore, we attempted to more precisely resolve the effects of modifying Lys^{326} and Lys^{328} by altering the acetylation reaction to favorably target these residues (Fig. S3). Based on previous measures of relative reactivities of actin lysines (38), we proceeded under the premise that performing the acetylation reaction with substoichiometric amounts of acetic anhydride would preferentially target Lys^{326} and Lys^{328}, and thus, any observed changes in Tpm-dependent inhibition of myosin binding could predominantly be attributed to modifying these residues. F-actin–Tpm *in vitro* motility was performed following treatment of actin with either sub- or suprastoichiometric amounts of acetic anhydride (Fig. 5*A*). Substoichiometric acetic anhydride

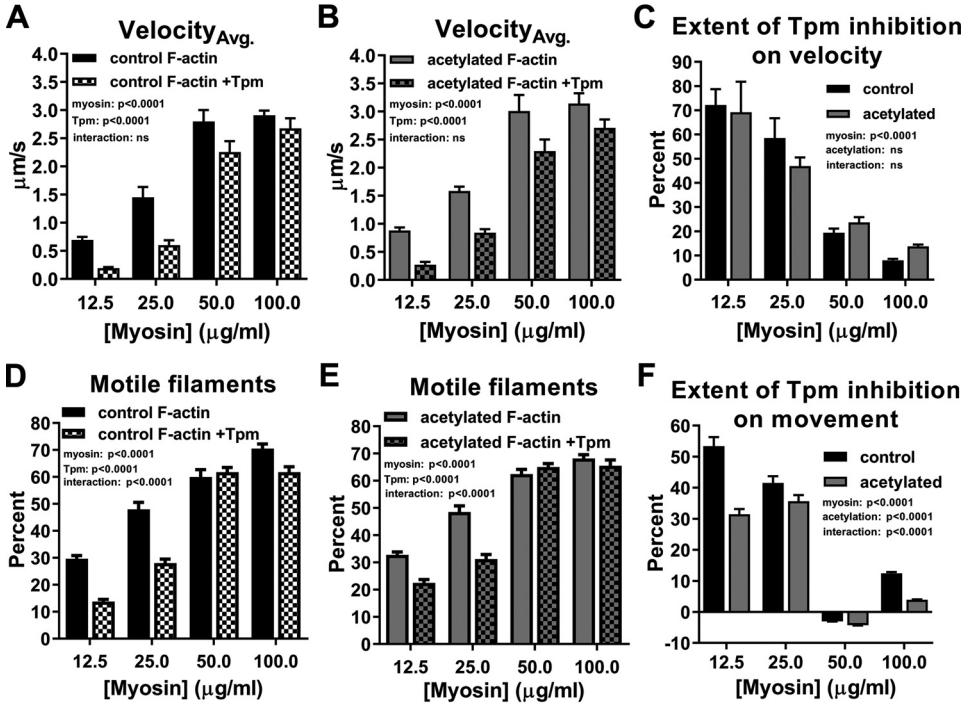

Figure 3. Actin acetylation reduces Tpm-based inhibition of actomyosin binding. *A* and *B*, control (*A*, *black*) and acetylated (*B*, *gray*) F-actin (*solid*) and F-actin–Tpm (*checkered*) velocities significantly increased as a function of myosin concentration, whereas Tpm addition significantly decreased velocities (two-way ANOVA; $p < 0.0001$; $n = 4$). *C*, percentage of decrease in control (*black*) and acetylated (*gray*) F-actin velocities observed as a result of Tpm addition revealed that acetylation had no significant effect on Tpm-mediated reduction of velocity (two-way ANOVA; $n = 4$). *D–F*, the effects of myosin concentration and Tpm on percentage of moving control (*D*, *black*) and acetylated (*E*, *gray*) F-actin (*solid*) and F-actin–Tpm (*checkered*) mirrored those on velocity, whereas actin acetylation (*F*, *gray*) significantly decreased Tpm-based inhibition of filament motion relative to control (*black*) (two-way ANOVA; $p < 0.0001$; $n = 17–22$).

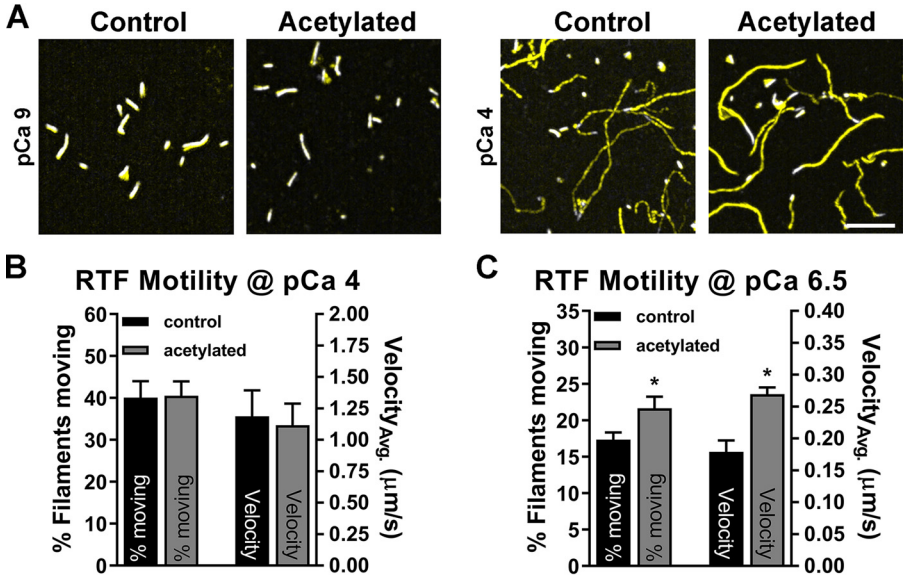

Figure 4. Reduced Tpm-based inhibition persists in acetylated actin-containing RTFs. *A*, representative images illustrating immeasurable (pCa 9) and equivalent (pCa 4) movement of control and acetylated actin-containing RTFs by overlaying the first frame of a 17–20-s movie (*white*) with a summative image of total motion (*yellow*). *Scale bar*, 7 μM. *B*, percentage of filaments moving (*left*; $n = 9$) and average velocities (*right*; $n = 2$) of control (*black*; 40.1 ± 3.9% and 1.19 ± 0.21 μM/s, respectively) and acetylated (*gray*; 40.5 ± 3.4% and 1.11 ± 0.17 μM/s, respectively) RTFs at pCa 4 were indistinguishable (two-tailed *t test*). *C*, percentage of filaments moving (*left*; $n = 7$) and average velocities (*right*; $n = 2$) of acetylated (24.75 ± 1.63% and 0.27 ± 0.01 μM/s, respectively) RTFs were significantly greater than control (20.11 ± 1.45% and 0.18 ± 0.02 μM/s, respectively) at pCa 6.5 (two-tailed *t* test; *, $p < 0.05$).

treatment resulted in significantly greater ($p < 0.001$) F-actin–Tpm movement relative to control. Furthermore, movement of F-actin–Tpm containing substoichiometric-treated actin was statistically equivalent to F-actin–Tpm movement containing suprastoichiometric-treated actin (Fig. 5*A*). Therefore, actin acetylation with substoichiometric levels of acetic anhydride that favors Lys^{326} and Lys^{328} acetylation recapitulates the impact of actin treated with suprastoichiometric levels of acetic anhydride, which is less discriminate. This might indicate that Lys^{326} and/or Lys^{328}

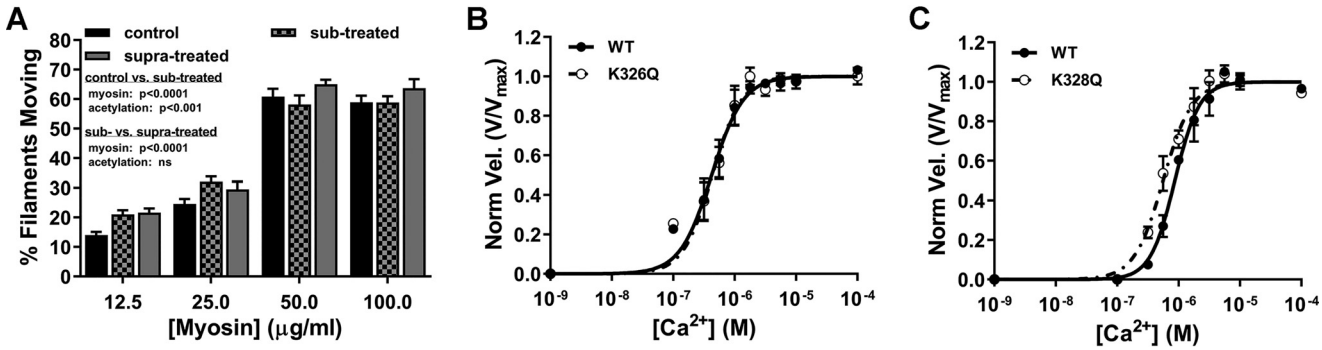

Figure 5. Lys^{328} pseudoacetylation enhances RTF Ca^{2+} sensitivity. *A*, treatment of actin with a substoichiometric amount of acetic anhydride (*checkered gray*) significantly increased percentage of actin–Tpm filaments moving relative to control (*black*) (two-way ANOVA; $p < 0.001$; $n = 9$–12), whereas substoichiometric-treated F-actin–Tpm movement was not significantly different from suprastoichiometric-treated (*gray*) (two-way ANOVA, $n = 10$–12). *B* and *C*, velocity-normalized plots of Ca^{2+}-dependent activation of K326Q- and K328Q-containing RTFs relative to respective WT controls. K326Q and K328Q maximum velocities ($V_{max} = 4.1 \pm 0.1$ and 3.3 ± 0.06 μM/s, respectively) did not significantly differ from respective internal WT controls ($V_{max} = 4.2 \pm 0.09$ and 3.3 ± 0.06 μM/s, respectively). *B*, Ca^{2+}-dependent activation of K326Q-containing RTFs was equivalent to WT control actin-containing RTFs as revealed by no significant differences in Ca^{2+} sensitivity ($[Ca^{2+}]_{50} = 0.43 \pm 0.029$ *versus* 0.42 ± 0.027 μM, respectively) or cooperativity ($h = 1.8 \pm 0.25$ *versus* 1.7 ± 0.21, respectively). *C*, although there was no significant change in cooperativity of K328Q-containing RTFs ($h = 1.8 \pm 0.21$) relative to WT control ($h = 2.2 \pm 0.22$), K328Q-containing RTF Ca^{2+} sensitivity ($[Ca^{2+}]_{50} = 0.56 \pm 0.032$ μM) was significantly increased relative to WT control ($[Ca^{2+}]_{50} = 0.87 \pm 0.044$ μM) ($p < 0.0001$; $n = 4$).

acetylation preferentially contributes to the observed increases in the percentage of F-actin–Tpm movement and RTF movement and velocity, which is in agreement with corroborating structural and *in silico* modeling data of the F-actin–Tpm interface (12, 15, 17–19, 25, 26). Hence, actin Lys^{326} and/or Lys^{328} modification specifically may modulate regulation of filaments replete with Tn–Tpm complexes.

Drosophila serves as a vehicle for transgenic actin production that can be purified in ample amounts needed for *in vitro* studies (22, 49, 54). The Act88F IFM actin isoform shares 92% identity with human vertebrate skeletal actin, and previous *in vitro* studies have confirmed that the two behave indistinguishably *in vitro* (22, 55). Similarly, the Act57B cardiac actin isoform is 93% identical to human vertebrate cardiac actin. To unambiguously assess the site-specific impact of Lys^{326} or Lys^{328} modification on Ca^{2+}-dependent thin filament regulation, we created transgenic *Drosophila* fly lines that express WT, K326Q, or K328Q Ac-mimetic (charge-neutralizing, yet sterically similar) Act57B actin in the IFM (30). Transgenic actin comprised roughly 15% of total IFM actin (Fig. S4), which was isolated and reconstituted into thin filaments using vertebrate cardiac Tn and Tpm. Ca^{2+} responsiveness of *Drosophila* actin-containing RTFs was determined via regulated *in vitro* motility at 100 μg/ml myosin as described previously (22). Maximum velocities of RTFs containing transgenic pseudoacetylated actin did not deviate more than 3% from respective transgenic WT actin-containing RTFs (Fig. 5, *B* and *C*). Furthermore, K326Q actin-containing RTFs exhibited no change in Ca^{2+} sensitivity ($[Ca^{2+}]_{50} = 0.43 \pm 0.029$ μM) or cooperativity ($h = 1.8 \pm 0.25$) relative to WT ($[Ca^{2+}]_{50} = 0.42 \pm 0.027$ μM and $h = 1.7 \pm 0.21$) (Fig. 5*B*). However, K328Q actin-containing RTFs were significantly hypersensitive ($p < 0.0001$) to Ca^{2+} ($[Ca^{2+}]_{50} = 0.56 \pm 0.032$ μM) relative to WT ($[Ca^{2+}]_{50} = 0.87 \pm 0.044$ μM), with no change in cooperativity ($h = 1.8 \pm 0.21$ and 2.2 ± 0.22, respectively) (Fig. 5*C*). Increased Ca^{2+} sensitivity in K328Q actin-containing RTFs is noteworthy for three reasons: 1) it is consistent with our previous data indicating increased myosin binding to acetylated F-actin–Tpm and RTFs at submaximal Ca^{2+} (Figs. 3 and 4); 2) it suggests that Lys^{328} acetylation alone is sufficient to cause Tpm mispositioning, and therefore less Ca^{2+} is required for RTF activation; and 3) it reveals the potential for Lys^{328} acetylation specifically to modulate and enhance thin filament Ca^{2+} sensitivity *in vivo*.

Discussion

This is the first study to assess the *in vitro* effects of actin acetylation on Tpm- and Tn–Tpm-mediated inhibition of actomyosin binding and cycling activity. Interestingly, *in vitro* chemical acetylation of F-actin appeared to have little effect on Tpm binding as determined by co-sedimentation assays. Because a previous study reported that the simultaneous substitution of actin Asp^{25}, Glu^{334}, Lys^{326}, and Lys^{328}, with alanines abolished F-actin–Tpm binding (19), we anticipated, *at a minimum*, a decrease in global Tpm binding affinity. However, no such reduction was observed under our experimental conditions. This discrepancy might be due to one or more of the following factors. First, negative effects on Tpm binding caused by alanine substitution–induced perturbations in the F-actin–Tpm topological landscape might exceed those elicited by either glutamine substitutions or Ac group transfer and charge neutralization. Second, relatively few positively charged Lys^{326} and/or Lys^{328} residues may be sufficient for collective Tpm binding. Third, disparities resulting from expression of recombinant rat striated α-Tpm and human smooth muscle actin compared with tissue-purified bovine cardiac Tpm and rabbit skeletal actin, as employed here, could differentially affect Tpm binding to the modified actins (16, 19, 20, 56, 57). Fourth, positively charged arginines on actin potentially minimize the loss in binding caused by lysine charge neutralization. Last, negatively charged Asp^{25} and/or Glu^{334} are also important contributors to global F-actin–Tpm binding affinity. Discriminating among these and additional possible mechanisms will require further investigation.

According to the results obtained using our *in vitro* motility protocol, acetylation had no effect on rabbit skeletal F-actin sliding speeds across all concentrations of rabbit skeletal

myosin tested. This corroborates the notion that the modification does not overtly impact actomyosin interactions and cross-bridge turnover rate in the absence of Tpm (Fig. 1*D*). In the presence of the regulatory strand, however, the number of motile actin–Tpm filaments significantly increased relative to control (Fig. 3, *D–F*), and the increase was significant under conditions that favored pan-acetylation of actin lysines or, potentially, under that which favored modification of only Lys^{326} and Lys^{328} (38) (Fig. 5*A*). These findings added credence to the thought that Lys^{326} and/or Lys^{328} modification might mitigate the ability of Tpm to inherently block myosin binding to actin.

Hyperacetylation of actin did not adversely affect thin filament stability or trigger disassembly because increasing actin acetylation ~290-fold did not hamper *in vitro* reconstitution of or render RTFs unresponsive to Ca^{2+}. Acetylated actin-containing RTF motility was completely absent at pCa 9 (Fig. 4*A*) and comparable with control RTFs at pCa 4 (Fig. 4, *A* and *B*). Therefore, at steady state, and in the presence of low or maximal Ca^{2+} (58–60), acetylation did not seemingly impact Tn's ability to bind F-actin–Tpm and establish the thin filament regulatory B- or M-states. However, at submaximal, activating pCa 6.5, both the percentage of motile and average velocity of acetylated actin-containing RTFs were significantly higher than control (Fig. 4*C*), consistent with reduced inhibition of myosin binding. Thus, despite a loss in positive surface charge, acetylated actin was capable of reconstituting into, and forming the molecular backbone of, a Ca^{2+}-responsive thin filament that evidently is hypersensitive to Ca^{2+} as indicated by increased myosin recruitment and propulsion speed at pCa 6.5.

Based on F-actin–Tpm results supporting the idea that Lys^{326} and/or Lys^{328} actin acetylation was largely responsible for attenuating Tpm-based inhibition (Fig. 5*A*), we reconstituted thin filaments containing Ac-mimetic K326Q or K328Q actin and tested the residue-specific effects of the modification on Ca^{2+} regulation of motility by measuring maximum sliding speeds, Ca^{2+} sensitivity, and cooperativity of activation (Fig. 5, *B* and *C*). We found that RTFs containing ~15% K328Q pseudoacetylated actin (30) were hypersensitive to Ca^{2+} (Fig. 5*C*). Enhanced Ca^{2+} sensitivity is consistent with increased acetylated F-actin–Tpm movement (Fig.'s 3, 5A) and enhanced activation of acetylated actin-containing RTFs at intermediate Ca^{2+} (Fig. 4*C*). Mechanistically, each result can be explained by either an actin acetylation- or K328Q-induced loss in Tpm-based inhibition of myosin binding.

Although Lys^{326} acetylation is not disqualified as a modifier of thin filament Ca^{2+} sensitivity, our results suggest that relative to Lys^{328}, Lys^{326} acetylation is, *at the very least*, significantly less impactful when present in RTFs at the tested amount. This is supported by our previous *in vivo* results that evaluated the specific effects of K326Q and K328Q Ac-mimetic actin on *Drosophila* flight ability and IFM morphology (30). Flies that ectopically expressed K328Q actin in IFMs, at roughly the same proportion present in RTFs here, were rendered flightless because of muscle destruction caused by severe, myosin-dependent hypercontraction. On the other hand, whereas the flight ability of K326Q-containing flies was significantly reduced, gross morphological structure of the IFMs was preserved. Therefore, when present at comparable levels in muscle, K328Q elicited a far more severe phenotype than K326Q actin, which suggests that the relative influence of Lys^{328} pseudoacetylation on the regulation of striated muscle contraction exceeds that of Lys^{326}. Our *in vitro* study corroborates the *in vivo* data and reveals a potential molecular mechanism to explain the exacerbated K328Q muscular phenotype. Relative to WT and K326Q, Lys^{328} pseudoacetylation of actin increases myosin binding to thin filaments because of elevated Ca^{2+} sensitivity and a greater loss in Tpm-based inhibition. These effects likely result in dysregulation of force production *in vivo*, which elicits destruction of IFMs; muscles that are particularly sensitive to perturbation.

Previous work has demonstrated a correlation between myofilament and myofibrillar protein acetylation levels and muscle function (35, 37); however, individual contributions from the various modified proteins to overall behavior remain, for the most part, unknown. One study reported that enzyme-mediated lysine acetylation of striated muscle myosin *in vitro* increases actomyosin affinity and F-actin sliding velocity, suggesting an acetylation-dependent enhancement in cross-bridge cycling (61). In contrast, our data suggest that actin acetylation does not appreciably affect actomyosin activity except when Tpm is present. Recently, we found that introduction of cardiac TnI Ac-mimetic K132Q decreased Ca^{2+} sensitivity of both RTFs and isolated myofibrils (62). In comparison, K328Q actin increased RTF Ca^{2+} sensitivity. Future work should focus on how acetylation of other known targets in muscle, *e.g.* TnT, TnC, titin, etc., individually and in combination, affect actomyosin activity and muscle performance (32).

Given both the Ac reactivity and functional importance of actin Lys^{328} (30, 38), it will be important to determine whether its acetylation status is sensitive to changes in cellular Ac-CoA levels, either physiological (*e.g.* feeding/fasting) or pathological (*e.g.* heart failure (63, 64)). Alternatively, increased/decreased KAT or KDAC enzymatic activity could alter levels of the PTM via a residue-specific mechanism. Although a number of small-molecule compounds have been shown to affect Ac-CoA tissue levels by inhibiting Ac-CoA carboxylase (65–68), discovery of specific KAT and/or KDAC activators/inhibitors that preferentially target sarcomeric actin, and in particular Lys^{326} and/or Lys^{328}, has been absent.

Ultimately, it will be informative to assess the site-specific stoichiometry of acetylation on actin, both *in vitro* and *in vivo*. Preliminary assessments by targeted parallel reaction monitoring MS are qualitatively consistent with Lys^{326} and Lys^{328} as highly reactive acetylation sites on actin,[1] as reported previously (30, 38). However, rigorous absolute quantitation at all previously reported acetylation sites on actin is technically challenging because of the presence of easily oxidized cysteine and methionine residues flanking many of the acetylation sites (Table 1). Nevertheless, site-specific actin Ac-peptide assays are in development.

In conclusion, notwithstanding the apparent marginal impact of actin acetylation on global F-actin–Tpm binding

[1] Anthony Cammarato and D. Brian Foster, unpublished observations.

affinity and stoichiometry, it reduced Tpm's ability to block actomyosin interactions and sensitized RTFs bathed in a submaximal, activating amount of Ca^{2+}. Site-specific mimicry of acetylation at the reactive residue, Lys^{328} on actin, is sufficient to recapitulate the Ca^{2+} sensitization of RTF activation. We submit that the physiological acetylation status of Lys^{328} and its susceptibility to change, in the context of disease, warrant further scrutiny because the PTM may serve as a potent modulator of striated muscle contraction.

Experimental procedures

Molecular modeling

Actin–myosin–Tpm and actin–Tpm structures were generated using Chimera version 1.9 (69) derived from Protein Data Bank codes 4A7f (41) and 9PDB file provided in Orzechowski *et al.* (12).

Drosophila stocks and husbandry

All flies were raised at 25 °C on a standard cornmeal–yeast–sucrose–agar medium. The *Act88F-Gal4* line was a gift from Dr. Richard M. Cripps (University of New Mexico, Albuquerque, NM, USA), and flies containing one of the *UAS-Act57B* actin transgenes (*UAS-Act57B*$^{GFP.WT}$, *UAS-Act57B*^{WT}, *UAS-Act57B*^{K326Q}, or *UAS-Act57B*^{K328Q}) were generated as described previously (30). Virgin *Act88F-Gal4* female flies were crossed with males containing one of the *UAS-Act57B* transgenes to create progeny that overexpressed transgenic $Act57B^{WT}$, $Act57B^{K326Q}$, or $Act57B^{K328Q}$ actin specifically in the IFM.

Protein sources, preparation, and quantitation

Lyophilized rabbit skeletal actin was obtained from Cytoskeleton (catalog no. AKL95). Psoas muscle myosin was purified (70) from white New Zealand rabbits provided by Dr. David Kass (Johns Hopkins University). Tissue-purified porcine cardiac Tpm was provided by Dr. Jeff Moore (University of Massachusetts–Lowell), and bovine cardiac isoforms of Tpm and Tn were provided by Dr. Larry Tobacman (University of Illinois at Chicago). Pools containing ectopically expressed $Act57B^{WT}$, $Act57B^{K326Q}$, or $Act57B^{K328Q}$ actin were purified from *Drosophila* IFMs according to previously published protocols (22, 49, 54).

In vitro actin acetylation and quantitation of lysine acetylation levels

In vitro actin acetylation was performed as described in Hitchcock-DeGregori *et al.* (38). 10 mg/ml globular (G-) actin, rehydrated as per manufacturer's instructions in 5 mM Tris-HCl, pH 8.0, 0.2 mM $CaCl_2$, 0.2 mM ATP, 5% (w/v) sucrose, and 1% (w/v) dextran, was distributed into 10 μl aliquots, flash-frozen in liquid nitrogen, and stored at −80 °C. Thawed G-actin was diluted 10-fold in low-salt buffer (25 mM KCl, 4 mM $MgCl_2$, 1 mM EGTA, 25 mM imidazole, pH 7.2, 10 mM DTT, 1 mM ATP) and polymerized for ∼1 h at room temperature. Stock acetic anhydride (Sigma–Aldrich lot no. SHBJ2093) was diluted 1:70 (4-fold ratio of total moles of acetic anhydride:total actin lysines) or 1:5600 (0.05 total mol of acetic anhydride:total actin lysines) in 100% acetonitrile and added to 96 μl of 1 mg/ml F-actin via addition of four 0.3 μl aliquots every 3 min with continuous agitation. Actins were stored at 4 °C overnight and dialyzed twice in the cold room against 1 liter of buffer (100 or 200 mM KCl, 5 mM $MgCl_2$, 5 mM Tris-HCl, pH 7.5) for at least 4 h to remove unreacted acetic anhydride.

Dialyzed acetylated actin was prepared in 4× lithium dodecyl sulfate sample buffer (Invitrogen lot no. 1920134), and ∼3 μg was loaded onto a 4–15% gradient SDS-PAGE gel (Bio-Rad catalog no. 456-1086). Proteins were transferred to a nitrocellulose membrane, blocked for 1 h in 1:1 mixture of TBS with 0.1% Tween 20 (Sigma lot no. SLBD6080V) and blocking buffer (LI-COR catalog no. 927-40000), and probed with anti–Ac-lysine (Cytoskeleton catalog no. AAC-03) antibodies, diluted 1:750 in TBS, for 1 h at room temperature or overnight in the cold room. Following four or five washes in TBS with 0.1% Tween 20 (TBST), Ac-lysine–bound primary antibodies were conjugated to 1:10,000 green secondary antibodies (LI-COR Biosciences) via 1 h incubation at room temperature. After numerous TBST washes, the membranes were exposed to a 1:7500 diluted anti-actin primary antibody (Proteintech catalog no. 20536-1-AP) at room temperature for 1 h, washed, and conjugated to 1:10,000 diluted red secondary antibodies (LI-COR Biosciences). Unconjugated antibodies were washed, and membranes were imaged on a LI-COR Odyssey fluorescence imager. Anti–Ac-lysine intensities were normalized to actin, and the average fold increase in actin-normalized lysine acetylation was determined for 9–11 individual measures.

Sample peptide preparation, chromatography, MS, and data analysis

48 μl of 1 mg/ml F-actin (25 mM KCl, 4 mM $MgCl_2$, 1 mM EGTA, 25 mM imidazole, pH 7.2, 10 mM DTT, 1 mM ATP) were aliquoted into two separate tubes. Each tube was mixed with either 100% acetonitrile or acetonitrile containing 1:140 (v/v) diluted stock acetic anhydride (Sigma–Aldrich lot no. SHBJ2093) via addition of four 0.3 μl aliquots every 3 min under constant mixing. Total moles of acetic anhydride added to the latter mixture was four times the number of actin lysines. F-actin samples were left at 4 °C overnight, and the following day ∼5 μg total protein were dried down, redissolved in 50 μl of 20 mM ammonium bicarbonate (pH 8.0), then reduced with 5 μl of 50 mM DTT at 55 °C for 1 h, and alkylated with 5 μl 50 mM iodoacetamide in the dark for 15 min. Enzymatic cleavage was performed with MS-grade trypsin/lys-C (Promega) at 37 °C overnight. The peptides were desalted with stage tips constructed from Empore C18 material (3M Corporation).

Tryptic peptides were subjected to nano-reversed phase HPLC coupled to MS/MS. Chromatography was conducted on a 75 μm × 250 mm column that was packed in-house into a PicoFrit self-pack (New Objective) with ReproSil-Pur C18-AQ (3 μM particles, 120 Å pores; Dr. Maisch, GmbH) and eluted with a 120 min linear two-solvent gradient (solvent A: 0.1% (v/v) formic acid (Suprapur, EMD Millipore) with in-house deionized, reverse-osmosed water; solvent B: 0.1% formic acid

in 80% (v/v) acetonitrile (Fisher Scientific) into an Orbitrap Fusion Lumos mass spectrometer equipped with the Easy-IC (internal calibration; Thermo Scientific) option. Data-dependent MS/MS acquisition was employed using a 3 s cycle time between MS scans. The resolution was 120,000 for MS and 30,000 for MS/MS. Signal targets were 2×10^6 ions in 60 s for MS and 5×10^4 ions in 54 s for MS/MS.

Acquired masses were searched against the RefSeq83 *Oryctolagus cuniculus* database using Mascot version 2.6.2 (Matrix Science), as implemented in Proteome Discoverer 1.4 (Thermo Scientific) with lysine acetylation (+42 Da), deamidation of asparagine and glutamine (+1 Da), and oxidation of methionine (+16 Da) included as variable search parameters. Carbamidomethyl cysteine (+57 Da) was set as a static search parameter. The precursor ion mass tolerance was set to 5 ppm, whereas 0.02 Da was used for MS/MS. Three missed cleavages were permitted. Data from Proteome Discoverer (1% false discovery rate) were imported into Scaffold Q+ v4.1.0 (Proteome Software) for conversion to mzIdentML and subsequent data inspection in Scaffold PTM v3.3.0 (Proteome Software). Lysine acetylation site confidence was assessed using Scaffold PTM's implementation of the A score (71).

F-actin–Tpm co-sedimentation

Dialyzed control and acetylated F-actin were diluted ~5-fold in buffer that yielded a final composition of 200 mM KCl, 2 mM $MgCl_2$, 10 mM Tris-HCl, pH 7.5, and 10 mM DTT. Stock Tpm concentration (65 μM) was determined via Bradford colorimetric assay (Bio-Rad), and 25 µl of F-actin (~3.5 µg) was mixed with minute volumes of porcine cardiac Tpm in duplicate at the following Tpm:actin molar ratios: 1:16, 1:15, 1:12, 1:10, 7:1, 1:5, 1:4, 1:3, 1:2, 1:1, 1.5:1, and 2:1. Mixtures were placed at room temperature for 30 min, then on ice for a minimum of 2 h, and spun down in a TLA-100 ultracentrifuge rotor at 100,000 rpm (436,000 × *g*) for 20 min at 4 °C. 12 µl of supernatant were added to 3 µl of 4× lithium dodecyl sulfate sample buffer (Invitrogen lot no. 1920134), whereas 15 µl of 1× sample buffer was added to the pellets. The samples were heated to ~90 °C for 3–5 min, centrifuged, loaded on a 4–15% gel (Bio-Rad catalog no. 456-1086), and run at 100 V for 1.5 h. The gels were stained overnight in G-250 Coomassie (Bio-Rad catalog no. 161-0786) and destained in double distilled water. In addition to assessment of F-actin–Tpm binding at "medium" ionic strength (*i.e.* 200 mM KCl), co-sedimentation experiments were equivalently performed under low (40 mM KCl, 4.2 mM $MgCl_2$, 0.8 mM EGTA, 20 mM imidazole, 1 mM Tris-HCl, pH 7.5, and 10 mM DTT) and high (500 mM KCl, 2 mM $MgCl_2$, 5 mM Tris-HCl, pH 7.5, 10 mM DTT) ionic strengths at 1:3 and 1:4 Tpm:actin molar ratios. KCl concentration was further increased to 820 mM (2 mM $MgCl_2$, 5 mM Tris-HCl, pH 7.5, 10 mM DTT), and F-actin–Tpm binding was determined at 1:2, 1:1, 1.5:1, and 2:1 Tpm:actin ratios.

Determination of F-actin–Tpm affinity

Coomassie-stained gels were scanned using a LI-COR Odyssey fluorescence imager, and band intensities were quantified using ImageStudio software. Known amounts of Tpm (0.5–6 µg) were used to plot a standard intensity curve to determine µg of Tpm in pellet and supernatant fractions and converted to moles (67 kDa). Negligible amounts of Tpm were found in pellet fractions in the absence of F-actin (Fig. S5). To determine moles of actin, relative amounts present in pellet and supernatant fractions were calculated by dividing intensities of each band by their sum. The amount of actin in pellet and supernatant fractions was then calculated by multiplying by total actin and converted to moles (42 kDa). Bound Tpm:actin molar ratios were plotted against free Tpm concentrations, and the data were fit to the Hill equation ($y = B_{max} \times x^h/(K_d{}^h + x^h)$) to derive B_{max} and K_d of Tpm for control and acetylated actin. Significant differences in fit parameters were assessed via extra sum of squares F-tests, with $p < 0.05$ deemed significant. The percentage of saturation of F-actin–Tpm binding was defined as the molar ratio of Tpm to actin in the pellet times 700.

F-actin, F-actin–Tpm, and RTF in vitro motility

A portion of dialyzed F-actin was diluted in low-salt buffer to ~1 μM and fluorescently labeled overnight via equimolar addition of Alexa 568 phalloidin (Ph) (Thermo Fisher catalog no. A12380). *In vitro* motility of control and acetylated Alexa 568 Ph-labeled F-actin was performed at myosin concentrations between 12.5 and 100 µg/ml at 30 °C, pH 7.2, and an ionic strength of 37 mM. Briefly, myosin was introduced into a flow cell and allowed 2 min to bind a nitrocellulose-coated coverslip. The surface was blocked with 2 mg/ml BSA, myosin "dead heads" were nonreversibly bound to unlabeled actin filaments, and enzymatically active myosin was bound to <10 nM Alexa 568 Ph-labeled F-actin. Fluorescent actin was excited and imaged using an X-CITE 120 LED lamp and 531/40 filter on an Olympus IX73 microscope. Emitted light was captured at 593/40 and detected on a Hamamatsu Flash 4LT EMCCD camera, operated with HCI imaging software. The videos were converted to multipage TIFs and imported into ImageJ for processing. Duplicate F-actin motility assessments from two separate suprastoichiometric acetylation reactions and one substoichiometric acetylation reaction were obtained in parallel with control F-actins. Videos from four to eight areas of each flow cell were recorded at 1–10 fps for 20 frames total, and the velocities of moving filaments were measured via automated tracking by ImageJ plugin *wrmtrack* (72). Average velocities and errors from two technical replicate experiments per biological replicate were calculated for filaments classified as movers (see supporting information). Total filaments analyzed per myosin concentration ranged between 250 and 2000.

Alexa 568 Ph-labeled F-actin was also incubated with 300 nM bovine cardiac Tpm on ice for at least 30 min prior to F-actin–Tpm motility. Motility buffer also included 150 nM Tpm to maintain Tpm saturation of F-actin. Average velocities and percent filaments moving of control and acetylated F-actin–Tpm samples were normalized to respective F-actin velocities and percentage of filaments moving at each myosin concentration. F-actin–normalized F-actin–Tpm motility parameters were subtracted from one and multiplied by 100 to determine the percentage of Tpm-based inhibition at each myosin concentration. The effect of acetylation on Tpm-based inhibition was

assessed via two-way ANOVA with $p < 0.05$ considered significant.

RTF motility at 25 μg/ml myosin was identically performed as F-actin–Tpm, except that 300 and 150 nM bovine cardiac Tn was added to F-actin–Tpm and Tpm-Ca^{2+}-containing motility buffers (50 mM KCl), respectively. Significant differences in average velocities and the percentage of moving filaments at pCa 4 and 6.5 between control and acetylated actin-containing RTFs were determined via two-tailed *t* tests with $p < 0.05$ considered significant. Ca^{2+}-regulated motility of RTFs containing *Drosophila*-derived, transgenic Act57B actin at 100 μg/ml myosin concentration was performed as described previously (22). Briefly, average RTF velocities calculated from two biological and two technical replicate experiments ($n = 4$) at each distinct [Ca^{2+}] were pooled and weighted based on the number of filaments analyzed for each of four replicate experiments. Pooled, raw velocity data were plotted as a function of [Ca^{2+}] and fit to the Hill equation to derive the V_{max} value for each RTF type. Average velocities at each [Ca^{2+}] were then normalized to each corresponding, Hill equation–derived V_{max}, and pooled normalized velocity *versus* [Ca^{2+}] data were refit to the Hill equation. Significant differences in $[Ca^{2+}]_{50}$ and cooperativity were determined via extra sum of squares F-tests between the fits.

Data availability

All data, associated protocols, methods, and sources of materials are available in the main text or in the supporting information. Additionally, the MS proteomics data have been deposited to the ProteomeXchange Consortium via the PRIDE (73) partner repository with the data set identifier PXD020732 and PXD019276.

Acknowledgments—We thank Dr.'s J. Moore (University of Massachusetts–Lowell) and L. S. Tobacman (University of Illinois at Chicago) for providing tissue-purified Tpm and Meera C. Viswanathan (Johns Hopkins University) and Dr. Anna Blice-Baum (Johns Hopkins University) for expert technical assistance. MS on acetylated actin was conducted by the Johns Hopkins University Mass Spectrometry Facility, for which we thank Robert O'Meally and Dr. Robert N. Cole.

Author contributions—W. S., D. B. F., and A. C. conceptualization; W. S., A. M., and D. B. F. data curation; W. S., D. B. F., and A. C. formal analysis; W. S., D. B. F., and A. C. validation; W. S., A. M., D. B. F., and A. C. investigation; W. S., D. B. F., and A. C. visualization; W. S., D. B. F., and A. C. methodology; W. S., A. M., D. B. F., and A. C. writing-original draft; W. S., D. B. F., and A. C. writing-review and editing; D. B. F. and A. C. resources; D. B. F. software; D. B. F. and A. C. supervision; D. B. F. and A. C. funding acquisition; D. B. F. and A. C. project administration.

Funding and additional information—This work was supported by National Institutes of Health Grants R01HL134821 (to D. B. F.) and R01HL124091 (to A. C.), American Heart Association Grants 18TPA34170575 (to D. B. F.) and 17POST33630159 (to W. S.), and a Johns Hopkins University Catalyst Award (to D. B. F.). The content is solely the responsibility of the authors and does not necessarily represent the official views of the National Institutes of Health.

Conflict of interest—The authors declare that they have no conflicts of interest with the contents of this article.

Abbreviations—The abbreviations used are: PTM, post-translational modification; Ac, Acetyl; Tpm, tropomyosin; Tn, troponin; F-, filamentous; RTF, reconstituted thin filament; TnI, inhibitory subunit of troponin; TnT, tropomyosin-binding subunit of troponin; TnC, calcium-binding subunit of troponin; B-state, blocking positional state of tropomyosin; C-state, closed positional state of tropomyosin; M-state, myosin-induced positional state of tropomyosin; A-state, "Apo" positional state of tropomyosin; IFM, indirect flight muscle; KAT, lysine acetylase; KDAC, lysine deacetylase; G-, globular; TBS, Tris-buffered saline; TBST, Tris-buffered saline with 0.1% Tween 20; Ph, phalloidin; ANOVA, analysis of variance.

References

1. Gordon, A. M., Homsher, E., and Regnier, M. (2000) Regulation of contraction in striated muscle. *Physiol. Rev.* **80,** 853–924 CrossRef Medline
2. Lehman, W. (2016) Thin filament structure and the steric blocking model. *Compr. Physiol.* **6,** 1043–1069 CrossRef Medline
3. McNamara, J. W., Li, A., Dos Remedios, C. G., and Cooke, R. (2015) The role of super-relaxed myosin in skeletal and cardiac muscle. *Biophys. Rev.* **7,** 5–14 CrossRef Medline
4. Trivedi, D. V., Adhikari, A. S., Sarkar, S. S., Ruppel, K. M., and Spudich, J. A. (2018) Hypertrophic cardiomyopathy and the myosin mesa: viewing an old disease in a new light. *Biophys. Rev.* **10,** 27–48 CrossRef Medline
5. Yamada, Y., Namba, K., and Fujii, T. (2020) Cardiac muscle thin filament structures reveal calcium regulatory mechanism. *Nat. Commun.* **11,** 153 CrossRef Medline
6. Hitchcock-DeGregori, S. E., and An, Y. (1996) Integral repeats and a continuous coiled coil are required for binding of striated muscle tropomyosin to the regulated actin filament. *J. Biol. Chem.* **271,** 3600–3603 CrossRef Medline
7. Hitchcock-DeGregori, S. E., Song, Y., and Greenfield, N. J. (2002) Functions of tropomyosin's periodic repeats. *Biochemistry* **41,** 15036–15044 CrossRef Medline
8. Singh, A., and Hitchcock-DeGregori, S. E. (2007) Tropomyosin's periods are quasi-equivalent for actin binding but have specific regulatory functions. *Biochemistry* **46,** 14917–14927 CrossRef Medline
9. Lorenz, M., Poole, K. J., Popp, D., Rosenbaum, G., and Holmes, K. C. (1995) An atomic model of the unregulated thin filament obtained by X-ray fiber diffraction on oriented actin–tropomyosin gels. *J. Mol. Biol.* **246,** 108–119 CrossRef Medline
10. Holmes, K. C., and Lehman, W. (2008) Gestalt-binding of tropomyosin to actin filaments. *J. Muscle Res. Cell Motil.* **29,** 213–219 CrossRef Medline
11. Li, X. E., Orzechowski, M., Lehman, W., and Fischer, S. (2014) Structure and flexibility of the tropomyosin overlap junction. *Biochem. Biophys. Res. Commun.* **446,** 304–308 CrossRef Medline
12. Orzechowski, M., Li, X. E., Fischer, S., and Lehman, W. (2014) An atomic model of the tropomyosin cable on F-actin. *Biophys. J.* **107,** 694–699 CrossRef Medline
13. Schmidt, W. M., Lehman, W., and Moore, J. R. (2015) Direct observation of tropomyosin binding to actin filaments. *Cytoskeleton (Hoboken)* **72,** 292–303 CrossRef Medline
14. Tobacman, L. S. (2008) Cooperative binding of tropomyosin to actin. *Adv. Exp. Med. Biol.* **644,** 85–94 CrossRef Medline
15. Li, X. E., Tobacman, L. S., Mun, J. Y., Craig, R., Fischer, S., and Lehman, W. (2011) Tropomyosin position on F-actin revealed by Em reconstruction and computational chemistry. *Biophys. J.* **100,** 1005–1013 CrossRef Medline

16. Heald, R. W., and Hitchcock-DeGregori, S. E. (1988) The structure of the amino terminus of tropomyosin is critical for binding to actin in the absence and presence of troponin. *J. Biol. Chem.* **263,** 5254–5259 Medline
17. Barua, B., Pamula, M. C., and Hitchcock-DeGregori, S. E. (2011) Evolutionarily conserved surface residues constitute actin binding sites of tropomyosin. *Proc. Natl. Acad. Sci. U.S.A.* **108,** 10150–10155 CrossRef Medline
18. Barua, B. (2013) Periodicities designed in the tropomyosin sequence and structure define its functions. *Bioarchitecture* **3,** 51–56 CrossRef Medline
19. Barua, B., Fagnant, P. M., Winkelmann, D. A., Trybus, K. M., and Hitchcock-DeGregori, S. E. (2013) A periodic pattern of evolutionarily conserved basic and acidic residues constitutes the binding interface of actin-tropomyosin. *J. Biol. Chem.* **288,** 9602–9609 CrossRef Medline
20. Lehman, W., Orzechowski, M., Li, X. E., Fischer, S., and Raunser, S. (2013) Gestalt-binding of tropomyosin on actin during thin filament activation. *J. Muscle Res. Cell Motil.* **34,** 155–163 CrossRef Medline
21. Rynkiewicz, M. J., Prum, T., Hollenberg, S., Kiani, F. A., Fagnant, P. M., Marston, S. B., Trybus, K. M., Fischer, S., Moore, J. R., and Lehman, W. (2017) Tropomyosin must interact weakly with actin to effectively regulate thin filament function. *Biophys. J.* **113,** 2444–2451 CrossRef Medline
22. Viswanathan, M. C., Schmidt, W., Rynkiewicz, M. J., Agarwal, K., Gao, J., Katz, J., Lehman, W., and Cammarato, A. (2017) Distortion of the actin A-triad results in contractile disinhibition and cardiomyopathy. *Cell Rep.* **20,** 2612–2625 CrossRef Medline
23. Orzechowski, M., Moore, J. R., Fischer, S., and Lehman, W. (2014) Tropomyosin movement on F-actin during muscle activation explained by energy landscapes. *Arch. Biochem. Biophys.* **545,** 63–68 CrossRef Medline
24. von der Ecken, J., Müller, M., Lehman, W., Manstein, D. J., Penczek, P. A., and Raunser, S. (2015) Structure of the F-actin–tropomyosin complex. *Nature* **519,** 114–117 CrossRef Medline
25. Brown, J. H., Zhou, Z., Reshetnikova, L., Robinson, H., Yammani, R. D., Tobacman, L. S., and Cohen, C. (2005) Structure of the mid-region of tropomyosin: bending and binding sites for actin. *Proc. Natl. Acad. Sci. U.S.A.* **102,** 18878–18883 CrossRef Medline
26. Greenfield, N. J., Huang, Y. J., Swapna, G. V., Bhattacharya, A., Rapp, B., Singh, A., Montelione, G. T., and Hitchcock-DeGregori, S. E. (2006) Solution NMR structure of the junction between tropomyosin molecules: implications for actin binding and regulation. *J. Mol. Biol.* **364,** 80–96 CrossRef Medline
27. Schmidt, W., and Cammarato, A. (2020) The actin "A-triad's" role in contractile regulation in health and disease. *J. Physiol.* **598,** 2897–2908 CrossRef Medline
28. Papadaki, M., Holewinski, R. J., Previs, S. B., Martin, T. G., Stachowski, M. J., Li, A., Blair, C. A., Moravec, C. S., Van Eyk, J. E., Campbell, K. S., Warshaw, D. M., and Kirk, J. A. (2018) Diabetes with heart failure increases methylglyoxal modifications in the sarcomere, which inhibit function. *JCI Insight* **3,** e121264 CrossRef
29. Meng, T., Bu, W., Ren, X., Chen, X., Yu, J., Eckenhoff, R. G., and Gao, W. D. (2016) Molecular mechanism of anesthetic-induced depression of myocardial contraction. *FASEB J.* **30,** 2915–2925 CrossRef Medline
30. Viswanathan, M. C., Blice-Baum, A. C., Schmidt, W., Foster, D. B., and Cammarato, A. (2015) Pseudo-acetylation of K326 and K328 of actin disrupts *Drosophila melanogaster* indirect flight muscle structure and performance. *Front. Physiol.* **6,** 116 CrossRef Medline
31. Lundby, A., Lage, K., Weinert, B. T., Bekker-Jensen, D. B., Secher, A., Skovgaard, T., Kelstrup, C. D., Dmytriyev, A., Choudhary, C., Lundby, C., and Olsen, J. V. (2012) Proteomic analysis of lysine acetylation sites in rat tissues reveals organ specificity and subcellular patterns. *Cell Rep.* **2,** 419–431 CrossRef Medline
32. Foster, D. B., Liu, T., Rucker, J., O'Meally, R. N., Devine, L. R., Cole, R. N., and O'Rourke, B. (2013) The cardiac acetyl-lysine proteome. *PLoS One* **8,** e67513 CrossRef Medline
33. Pougovkina, O., Te Brinke, H., Ofman, R., van Cruchten, A. G., Kulik, W., Wanders, R. J., Houten, S. M., and de Boer, V. C. (2014) Mitochondrial protein acetylation is driven by acetyl-CoA from fatty acid oxidation. *Hum. Mol. Genet.* **23,** 3513–3522 CrossRef Medline
34. Wagner, G. R., and Payne, R. M. (2013) Widespread and enzyme-independent N^{ϵ}-acetylation and N^{ϵ}-succinylation of proteins in the chemical conditions of the mitochondrial matrix. *J. Biol. Chem.* **288,** 29036–29045 CrossRef Medline
35. Gupta, M. P., Samant, S. A., Smith, S. H., and Shroff, S. G. (2008) HDAC4 and PCAF bind to cardiac sarcomeres and play a role in regulating myofilament contractile activity. *J. Biol. Chem.* **283,** 10135–10146 CrossRef Medline
36. Waltregny, D., Glénisson, W., Tran, S. L., North, B. J., Verdin, E., Colige, A., and Castronovo, V. (2005) Histone deacetylase HDAC8 associates with smooth muscle α-actin and is essential for smooth muscle cell contractility. *FASEB J.* **19,** 966–968 CrossRef Medline
37. Jeong, M. Y., Lin, Y. H., Wennersten, S. A., Demos-Davies, K. M., Cavasin, M. A., Mahaffey, J. H., Monzani, V., Saripalli, C., Mascagni, P., Reece, T. B., Ambardekar, A. V., Granzier, H. L., Dinarello, C. A., and McKinsey, T. A. (2018) Histone deacetylase activity governs diastolic dysfunction through a nongenomic mechanism. *Sci. Transl. Med.* **10,** eaao0144 CrossRef Medline
38. Hitchcock-De Gregori, S. E., Mandala, S., and Sachs, G. A. (1982) Changes in actin lysine reactivities during polymerization detected using a competitive labeling method. *J. Biol. Chem.* **257,** 12573–12580 Medline
39. Szilagyi, L., and Lu, R. C. (1982) Changes of lysine reactivities of actin in complex with myosin subfragment-1, tropomyosin and troponin. *Biochim. Biophys. Acta* **709,** 204–211 CrossRef Medline
40. Hitchcock-De Gregori, S. E. (1982) Study of the structure of troponin-I by measuring the relative reactivities of lysines with acetic anhydride. *J. Biol. Chem.* **257,** 7372–7380 Medline
41. Behrmann, E., Müller, M., Penczek, P. A., Mannherz, H. G., Manstein, D. J., and Raunser, S. (2012) Structure of the rigor actin–tropomyosin–myosin complex. *Cell* **150,** 327–338 CrossRef Medline
42. Landis, C. A., Bobkova, A., Homsher, E., and Tobacman, L. S. (1997) The active state of the thin filament is destabilized by an internal deletion in tropomyosin. *J. Biol. Chem.* **272,** 14051–14056 CrossRef Medline
43. Korman, V. L., and Tobacman, L. S. (1999) Mutations in actin subdomain 3 that impair thin filament regulation by troponin and tropomyosin. *J. Biol. Chem.* **274,** 22191–22196 CrossRef Medline
44. Butters, C. A., Willadsen, K. A., and Tobacman, L. S. (1993) Cooperative interactions between adjacent troponin–tropomyosin complexes may be transmitted through the actin filament. *J. Biol. Chem.* **268,** 15565–15570 Medline
45. Rome, L. C., Cook, C., Syme, D. A., Connaughton, M. A., Ashley-Ross, M., Klimov, A., Tikunov, B., and Goldman, Y. E. (1999) Trading force for speed: why superfast crossbridge kinetics leads to superlow forces. *Proc. Natl. Acad. Sci. U.S.A.* **96,** 5826–5831 CrossRef Medline
46. Månsson, A., Rassier, D., and Tsiavaliaris, G. (2015) Poorly understood aspects of striated muscle contraction. *Biomed. Res. Int.* **2015,** 245154 CrossRef Medline
47. Gerson, J. H., Bobkova, E., Homsher, E., and Reisler, E. (1999) Role of residues 311/312 in actin–tropomyosin interaction *in vitro* motility study using yeast actin mutant E311A/R312A. *J. Biol. Chem.* **274,** 17545–17550 CrossRef Medline
48. VanBuren, P., Palmiter, K. A., and Warshaw, D. M. (1999) Tropomyosin directly modulates actomyosin mechanical performance at the level of a single actin filament. *Proc. Natl. Acad. Sci. U.S.A.* **96,** 12488–12493 CrossRef Medline
49. Viswanathan, M. C., Schmidt, W., Franz, P., Rynkiewicz, M. J., Newhard, C. S., Madan, A., Lehman, W., Swank, D. M., Preller, M., and Cammarato, A. (2020) A role for actin flexibility in thin filament-mediated contractile regulation and myopathy. *Nat. Commun.* **11,** 2417 CrossRef Medline
50. Barua, B., Winkelmann, D. A., White, H. D., and Hitchcock-DeGregori, S. E. (2012) Regulation of actin–myosin interaction by conserved periodic sites of tropomyosin. *Proc. Natl. Acad. Sci. U.S.A.* **109,** 18425–18430 CrossRef Medline
51. Beuckelmann, D. J., Näbauer, M., and Erdmann, E. (1992) Intracellular calcium handling in isolated ventricular myocytes from patients with terminal heart failure. *Circulation* **85,** 1046–1055 CrossRef Medline
52. Piacentino, V., 3rd, Weber, C. R., Chen, X., Weisser-Thomas, J., Margulies, K. B., Bers, D. M., and Houser, S. R. (2003) Cellular basis of abnormal calcium transients of failing human ventricular myocytes. *Circ. Res.* **92,** 651–658 CrossRef Medline

53. Smith, G. L., and Eisner, D. A. (2019) Calcium buffering in the heart in health and disease. *Circulation* **139,** 2358–2371 CrossRef Medline
54. Razzaq, A., Schmitz, S., Veigel, C., Molloy, J. E., Geeves, M. A., and Sparrow, J. C. (1999) Actin residue Glu^{93} is identified as an amino acid affecting myosin binding. *J. Biol. Chem.* **274,** 28321–28328 CrossRef Medline
55. Bing, W., Razzaq, A., Sparrow, J., and Marston, S. (1998) Tropomyosin and troponin regulation of wild type and E93K mutant actin filaments from *Drosophila* flight muscle: charge reversal on actin changes actin-tropomyosin from on to off state. *J. Biol. Chem.* **273,** 15016–15021 CrossRef Medline
56. Li, X. E., Lehman, W., Fischer, S., and Holmes, K. C. (2010) Curvature variation along the tropomyosin molecule. *J. Struct. Biol.* **170,** 307–312 CrossRef Medline
57. Li, X. E., Holmes, K. C., Lehman, W., Jung, H., and Fischer, S. (2010) The shape and flexibility of tropomyosin coiled coils: implications for actin filament assembly and regulation. *J. Mol. Biol.* **395,** 327–339 CrossRef Medline
58. Berchtold, M. W., Brinkmeier, H., and Müntener, M. (2000) Calcium ion in skeletal muscle: its crucial role for muscle function, plasticity, and disease. *Physiol. Rev.* **80,** 1215–1265 CrossRef Medline
59. Kuo, I. Y., and Ehrlich, B. E. (2015) Signaling in muscle contraction. *Cold Spring Harb. Perspect. Biol.* **7,** a006023 CrossRef Medline
60. Chung, J. H., Biesiadecki, B. J., Ziolo, M. T., Davis, J. P., and Janssen, P. M. (2016) Myofilament calcium sensitivity: role in regulation of *in vivo* cardiac contraction and relaxation. *Front. Physiol.* **7,** 562 CrossRef Medline
61. Samant, S. A., Pillai, V. B., Sundaresan, N. R., Shroff, S. G., and Gupta, M. P. (2015) Histone deacetylase 3 (HDAC3)–dependent reversible lysine acetylation of cardiac myosin heavy chain isoforms modulates their enzymatic and motor activity. *J. Biol. Chem.* **290,** 15559–15569 CrossRef Medline
62. Lin, Y. H., Schmidt, W., Fritz, K. S., Jeong, M. Y., Cammarato, A., Foster, D. B., Biesiadecki, B. J., McKinsey, T. A., and Woulfe, K. C. (2020) Site-specific acetyl-mimetic modification of cardiac troponin I modulates myofilament relaxation and calcium sensitivity. *J. Mol. Cell. Cardiol.* **139,** 135–147 CrossRef Medline
63. Foster, D. B., Liu, T., Kammers, K., O'Meally, R., Yang, N., Papanicolaou, K. N., Talbot, C. C., Jr., Cole, R. N., and O'Rourke, B. (2016) Integrated omic analysis of a guinea pig model of heart failure and sudden cardiac death. *J. Proteome Res.* **15,** 3009–3028 CrossRef Medline
64. Bedi, K. C., Jr., Snyder, N. W., Brandimarto, J., Aziz, M., Mesaros, C., Worth, A. J., Wang, L. L., Javaheri, A., Blair, I. A., Margulies, K. B., and Rame, J. E. (2016) Evidence for intramyocardial disruption of lipid metabolism and increased myocardial ketone utilization in advanced human heart failure. *Circulation* **133,** 706–716 CrossRef Medline
65. Tong, L., and Harwood, H. J., Jr. (2006) Acetyl-coenzyme A carboxylases: versatile targets for drug discovery. *J. Cell. Biochem.* **99,** 1476–1488 CrossRef Medline
66. Svensson, R. U., Parker, S. J., Eichner, L. J., Kolar, M. J., Wallace, M., Brun, S. N., Lombardo, P. S., Van Nostrand, J. L., Hutchins, A., Vera, L., Gerken, L., Greenwood, J., Bhat, S., Harriman, G., Westlin, W. F., *et al.* (2016) Inhibition of acetyl-CoA carboxylase suppresses fatty acid synthesis and tumor growth of non-small-cell lung cancer in preclinical models. *Nat. Med.* **22,** 1108–1119 CrossRef Medline
67. Kim, C. W., Addy, C., Kusunoki, J., Anderson, N. N., Deja, S., Fu, X., Burgess, S. C., Li, C., Ruddy, M., Chakravarthy, M., Previs, S., Milstein, S., Fitzgerald, K., Kelley, D. E., and Horton, J. D. (2017) Acetyl CoA carboxylase inhibition reduces hepatic steatosis but elevates plasma triglycerides in mice and humans: a bedside to bench investigation. *Cell Metab.* 26, 576 CrossRef Medline
68. Lawitz, E. J., Coste, A., Poordad, F., Alkhouri, N., Loo, N., McColgan, B. J., Tarrant, J. M., Nguyen, T., Han, L., Chung, C., Ray, A. S., McHutchison, J. G., Subramanian, G. M., Myers, R. P., Middleton, M. S., *et al.* (2018) Acetyl-CoA carboxylase inhibitor GS-0976 for 12 weeks reduces hepatic *de novo* lipogenesis and steatosis in patients with nonalcoholic steatohepatitis. *Clin. Gastroenterol. Hepatol.* **16,** 1983–1991.e3 CrossRef Medline
69. Pettersen, E. F., Goddard, T. D., Huang, C. C., Couch, G. S., Greenblatt, D. M., Meng, E. C., and Ferrin, T. E. (2004) UCSF Chimera: a visualization system for exploratory research and analysis. *J. Comput. Chem.* **25,** 1605–1612 CrossRef Medline
70. Kron, S. J., and Spudich, J. A. (1986) Fluorescent actin filaments move on myosin fixed to a glass surface. *Proc. Natl. Acad. Sci. U.S.A.* **83,** 6272–6276 CrossRef Medline
71. Beausoleil, S. A., Villén, J., Gerber, S. A., Rush, J., and Gygi, S. P. (2006) A probability-based approach for high-throughput protein phosphorylation analysis and site localization. *Nat. Biotechnol.* **24,** 1285–1292 CrossRef Medline
72. Nussbaum-Krammer, C. I., Neto, M. F., Brielmann, R. M., Pedersen, J. S., and Morimoto, R. I. (2015) Investigating the spreading and toxicity of prion-like proteins using the metazoan model organism C. elegans. *J. Vis. Exp.* **95,** 52321 CrossRef Medline
73. Perez-Riverol, Y., Csordas, A., Bai, J., Bernal-Llinares, M., Hewapathirana, S., Kundu, D. J., Inuganti, A., Griss, J., Mayer, G., Eisenacher, M., Perez, E., Uszkoreit, J., Pfeuffer, J., Sachsenberg, T., Yilmaz, S., *et al.* (2019) The PRIDE database and related tools and resources in 2019: improving support for quantification data. *Nucleic Acids Res* **47,** D442–D450 CrossRef Medline
74. Groth, A. C., Fish, M., Nusse, R., and Calos, M. P. (2004) Construction of transgenic Drosophila by using the site-specific integrase from phage phiC31. *Genetics* **166,** 1775–1782 CrossRef Medline
75. Brand, A. H., and Perrimon, N. (1993) Targeted gene expression as a means of altering cell fates and generating dominant phenotypes. *Development* **118,** 401–415 Medline